Proceedings of the ASME 2018 37th International Conference on Ocean, Offshore and Arctic Engineering
OMAE2018
June 17-22, 2018, Madrid, Spain

OMAE2018-77671

DETECTION OF PLUNGING BREAKING WAVES BASED ON MACHINE LEARNING

Ying Tu*

Department of Civil and Environmental Engineering, NTNU
Trondheim, 7491
Norway
Email: ying.tu@ntnu.no

Zhengshun Cheng

Department of Marine Technology
AMOS and CeSOS, NTNU
Trondheim, 7491
Norway
Email:zhengshun.cheng@ntnu.no

Michael Muskulus

Department of Civil and Environmental Engineering, NTNU
Trondheim, 7491
Norway
Email: michael.muskulus@ntnu.no

ABSTRACT

Plunging breaking waves that occur in the vicinity of offshore structures can lead to high impulsive slamming loads, which are significant for the structural loading. The occurrence of plunging breaking waves is usually identified based on criteria that are derived from theoretical analyses and experimental studies. Given a large amount of data, detecting plunging breaking waves can be treated as a typical classification problem, which can be solved by a machine learning approach. In this study, logistic regression algorithm is used together with the experimental data from the WaveSlam project to train a classifier for the detection. Three normalized dimensionless features are introduced based on the measured data for the training. A classifier with respect to four wave parameters (i.e. water depth, wave height, crest height and wave period) is then explicitly developed for detecting plunging breaking waves. It is found that the trained classifier has an accuracy of 98.7% and F_1 score of 99.2% for the tested data. Among the three dimensionless parameters, the ratio of wave height to water depth, H/d, is the most decisive factor for the detection of plunging breaking waves.

INTRODUCTION

A breaking wave is a wave whose amplitude reaches a critical level at which it becomes unstable and dissipates large amounts of wave energy into turbulent kinetic energy. It may occur anywhere if the amplitude is sufficient, including in mid-ocean. However, it is particularly common in shallow water, e.g. on beaches. There are four basic types of breaking waves, i.e. spilling, plunging, collapsing and surging [1]. Among them, the plunging breaking wave is most relevant to slamming loads on offshore structures, for instance offshore wind turbine supporting structures.

A large amount of efforts has been devoted to identify the criteria for the occurrence of wave breaking and plunging breaking waves. The state-of-the-art wave breaking criteria and plunging criteria have been reviewed in [2]. These criteria are achieved by theoretical analyses, numerical simulations or experimental studies. The present study also deals with the detection of plunging breaking wave events, but without applying any existing criteria. A machine learning based approach is proposed and applied to detect the plunging breaking waves.

Machine learning is the field of study that gives computers the ability to learn without being explicitly programmed [3]. During the last decades, modern machine learning techniques have been proposed to train models that can provide good empirical models [4]. In the field of ocean engineering, machine learning has been employed to deal with a range of tasks, for instance predicting scour depth [5], wave forecasting [6–8] etc.

Machine learning has also been applied to predict the wave-breaking characteristics. Deo et al. [9] employed a neural network approach to predict the breaking wave height and water depth for waves transforming over a range of simply sloped bottoms. Akoz et al. [10] also employed artificial neural network to predict the geometrical properties of so-called perfect breaking

*Address all correspondence to this author.

wave (i.e. a wave breaks on a vertical wall with an almost vertical front face) on composite breakwaters. Kouvaras and Dhanak [11] extended the Deo et al. [9] approach to predict other characteristics of wave breaking, including the type of wave breaking, the position of breaking, the wave setup, and the rate of dissipation of wave energy.

All these studies [9–11] used the neural network approach. The neural network model used in [9] was trained using empirical graphs and equations. The neural network models used in [10, 11] were trained and tested by laboratory observations of regular breaking waves in small scale wave flumes. However, only a limited number of regular breaking waves were recorded and used in the studies by [10, 11], which implies that the training data set might be limited and thus might affect the prediction accuracy if the trained model is applied to predict the characteristics of breaking waves that are not within the range of training data set. Additionally, the neural network model does not provide a regression equation relating inputs and outputs.

In this study, a machine learning approach is used to detect the plunging breaking waves. Based on a series of measured regular breaking waves in a large wave flume, a logistic regression model is trained and used to identify breaking waves. Performance of the developed model is also evaluated.

DATA DESCRIPTION

The experimental data from the WaveSlam project [1] [12] are used for the analysis in this study. The project aims to study the slamming forces from plunging breaking waves on jacket structures, through experiment with a 1:8 scale model of a typical jacket structure used in offshore wind industry. The experiment was conducted using the Large Wave Flume facilities at the Coastal Research Centre (Forschungszentrum Küste, FZK) [2], Hannover, Germany.

The setup of the experiment is shown in Fig. 1. The wave flume is approximately 300m long, 5m wide and 7m deep. The waves were generated by the wave board at the left end of the flume, went over a 1:10 slope, then reached the jacket model on a plateau. The breaking waves were supposed to break at or close to the jacket model. The water depth at the jacket model was set to 2.0m or 1.8m.

A global coordinate system is defined as following: The origin is positioned at the middle position of the wave board (x = 0), at the bottom of the channel (z = 0) and at the south side of the flume, namely the right side when following the flow (y = 0). The x-axis is positive in the wave direction. The z-axis is positive upwards. The y-axis forms a right hand system with the other axes.

Wave gauges were installed at 15 different locations along the wave flume, and the motions of the wave paddle were recorded. The measurement of Wave Gauge S9 (WG S9) is used. This wave gauge is the first available one above the plateau after the slope, where the breaking waves were fully developed. The wave gauge is located in the plane of the front legs of the jacket model, and between the model and the south wall of the wave flume. The location of the gauge in the global coordinates is show in Table 1 and illustrated in Fig. 1. There were two more wave gauges located above the plateau, one after the front legs and the other at the back legs. However, the measurements from these two gauges were more prone to the disturbance from the jacket model, so they are not used.

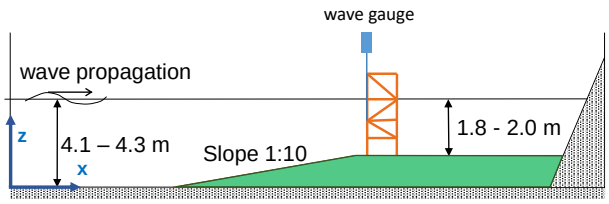

FIGURE 1. Setup of the experiment.

TABLE 1. Location of the used wave gauge.

Channel name	Description	x [m]	y [m]	z [m]
WG S9	WG front column	198.37	0.60	7.00

A list of regular wave test cases used in the analysis is given in Table 2. There are 66 test cases and in each test, more than one run may be conducted. These test cases consist of different combinations of wave height, wave period and water depth. Wave height varies from 0.75 m to 1.9 m, and wave period ranges from 3.0 s to 5.55 s. It should be noted that the wave height and wave period given in Table 2 are inputs to the wave paddle. The wave height experienced by the WG S9 and the structure are expected to be larger than that at the wave paddle due to the slope.

For each test, whether the regular waves are breaking or not is also highlighted in Table 2. They are identified based on visual observations from the experiment. The sampling frequency of wave gauges was 100 Hz or 200 Hz, depending on wave cases.

METHODS

Plunging breaking waves, which can cause slamming loads on offshore structures, have an on/off feature. Therefore, it is a typical binary classification problem in supervised machine learning, to distinguish plunging breaking waves and non-breaking ones. Classification refers to the problem to classify examples into given set of categories. The two categories here are breaking and non-breaking.

[1] http://hydralab.eu/research--results/ta-projects/project/19/; January 2018
[2] https://www.fzk.uni-hannover.de/; January 2018

TABLE 2. Selected regular wave test cases. The wave height and period are inputs to the wave paddle. The water depth is also nominal at the wave paddle. The water depth at the structure equals to the nominal water depth at the wave paddle minus the height of the plateau 2.3m. Each run of Tests 64-66 has 10 waves. Each run of the other tests has 20 waves. In each run of each test, there is one wave that is not used for the analysis (see Section Data pre-processing).

Test No.	No. of runs	Wave height [m]	Wave period [s]	Depth [m]	Breaking?	Test No.	No. of runs	Wave height [m]	Wave period [s]	Depth [m]	Breaking?
1	2	1.00	3.00	4.3	N	34	1	1.80	5.55	4.3	Y
2	1	1.10	3.00	4.3	N	35	1	1.50	5.55	4.3	Y
3	1	1.20	3.00	4.3	N	36	1	1.40	5.55	4.3	Y
4	1	1.30	3.00	4.3	N	37	1	1.30	5.55	4.3	Y
5	1	1.35	3.00	4.3	Y	38	1	1.45	4	4.3	Y
6	1	1.35	4.00	4.3	Y	39	1	1.55	4	4.3	Y
7	1	1.45	4.00	4.3	Y	40	1	1.65	4	4.3	Y
8	1	1.55	4.00	4.3	Y	41	1	1.70	5.55	4.3	Y
9	1	1.65	4.00	4.3	Y	42	1	1.70	5.2	4.3	Y
10	1	1.60	4.00	4.3	Y	43	1	1.65	4.9	4.3	Y
11	1	1.40	4.6	4.3	Y	44	1	1.35	4.6	4.3	Y
12	1	1.50	4.6	4.3	Y	45	1	1.70	4.6	4.3	Y
13	1	1.30	4.6	4.3	Y	46	5	1.70	5.2	4.3	Y
14	1	1.60	4.6	4.3	Y	47	5	1.50	4.9	4.3	Y
15	1	1.65	4.6	4.3	Y	48	5	1.40	4.6	4.3	Y
16	2	1.70	4.6	4.3	Y	49	1	1	4	4.3	N
17	1	1.75	4.6	4.3	Y	50	1	1	4.6	4.3	N
18	1	1.45	4.9	4.3	Y	51	1	1	4.9	4.3	N
19	1	1.30	4.9	4.3	Y	52	1	1	5.2	4.3	N
20	1	1.40	4.9	4.3	Y	53	1	1	5.55	4.3	N
21	1	1.50	4.9	4.3	Y	54	1	0.75	4	4.3	N
22	1	1.60	4.9	4.3	Y	55	1	0.75	4.6	4.3	N
23	1	1.70	4.9	4.3	Y	56	1	0.75	5.2	4.3	N
24	1	1.75	4.9	4.3	Y	57	1	0.75	5.55	4.3	N
25	1	1.80	4.9	4.3	Y	58	3	1.4	3	4.1	Y
26	1	1.40	5.2	4.3	Y	59	3	1.7	4	4.1	Y
27	1	1.30	5.2	4.3	Y	60	3	1.8	4.6	4.1	Y
28	1	1.50	5.2	4.3	Y	61	3	1.8	4.9	4.1	Y
29	1	1.60	5.2	4.3	Y	62	2	1.85	5.2	4.1	Y
30	1	1.70	5.2	4.3	Y	63	3	1.85	5.55	4.1	Y
31	1	1.80	5.2	4.3	Y	64	2	1.8	5.2	4.3	Y
32	1	1.60	5.55	4.3	Y	65	5	1.9	5.2	4.3	Y
33	1	1.70	5.55	4.3	Y	66	5	1.9	5.55	4.3	Y

A typical classification problem is demonstrated by Fig. 2. Labeled training data are first fed into a machine learning algorithm to obtain a classification rule. Then, the classification rule is applied to new data to make predictions.

For our investigated problem specifically, the work flow is illustrated in Fig. 3. The major blocks of the work flow are explained in detail below.

Data pre-processing

The measured wave elevation is first pre-processed. For each run in each test, a band-pass filter is applied to remove the high-frequency noise in the measured wave elevations. During each run, 20 (or 10) regular waves were recorded; however, only 19 (or 9) regular waves are found to have similar wave height, and are thus selected for further analysis. As a result, a total of 1780 regular waves are extracted from the measured data.

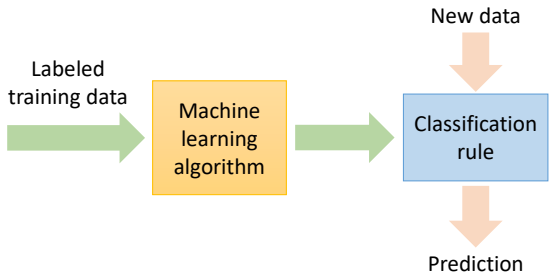

FIGURE 2. Illustration of classification problem.

Feature extraction

A perfect regular wave can be represented by water depth d, wave height H, crest height η_p, trough height η_t, and wave period T. However, the measured regular waves are not "perfect", since the measured regular waves in the same run differ slightly. A representative measured wave elevation at WG S9 is illustrated in Fig. 4. The following procedure is used to extract the key parameters for each regular wave. For the i^{th} regular wave, the crest height η_{p_i} and wave period estimated from two neighboring troughs T_{t_i} are marked in Fig. 4. The wave period estimated from neighboring peaks is estimated by $T_{p_i} = (T_i + T_{i+1})/2$, and the trough height estimated from neighboring troughs is calculated by $\eta_{t_i} = (\eta_i + \eta_{i+1})/2$. The wave height is thus expressed as $H_i = \eta_{p_i} + \eta_{t_i}$. Therefore, the features extracted from each regular wave are water depth d, wave height H, crest height η_p, trough height η_t, wave peak period T_p and wave trough period T_t.

Labeling

Each wave sample is labeled as positive class 1 or negative class 0, representing breaking or non-breaking, respectively, according to the wave cases described in Table 2.

Data splitting

The processed and labeled data are randomly shuffled and divided into two data sets: training set, which is composed of 70% of the total data, and testing set, which is composed of 30% of the total data.

Feature normalization

The extracted features might be combined (e.g. divided, multiplied) into new features to be used in the machine learning algorithm. The scale of the various features can vary largely. Using features with large difference in scale may cause instability in the learning algorithm. Therefore, it is important to normalize the features.

Feature normalization is carried out separately for the training set and for the testing set. Assuming there are m samples (waves) and n features in a data set (training set or testing set), we introduce $x_j^{(i)}$ to represent the value of the jth feature of the ith sample. The values of the jth feature from all the samples are written in a vector form as

$$\mathbf{x_j} = \left[x_j^{(1)}\ x_j^{(2)}\ \dots\ x_j^{(m)}\right]^T \tag{1}$$

The normalized values of the jth feature from all the samples are written as

$$\lambda_\mathbf{j} = [\lambda_j^{(1)}\ \lambda_j^{(2)}\ \dots\ \lambda_j^{(m)}]^T \tag{2}$$

which is calculated by

$$\lambda_\mathbf{j} = \frac{\mathbf{x_j} - \mu_j}{\sigma_j} \tag{3}$$

where μ_j and σ_j are the mean and the standard deviation calculated from $\mathbf{x_j}$ of the training set, respectively. The same values are applied to the normalization of the corresponding features in the testing set.

For each data set, the aforementioned labels are also written in a vector form as

$$\mathbf{y^{(i)}} = \left[y^{(1)}\ y^{(2)}\ \dots\ y^{(m)}\right]^T \tag{4}$$

Training

Commonly used machine learning algorithms for classification problems include logistic regression, support vector machine, decision tree and more advanced artificial neutral network. We tested support vector machine with linear and Gaussian kernels, decision tree, logistic regression, as well as some ensemble learnings. The logistic regression algorithm [13] is found to deliver as accurate results as the more advanced algorithms for our purpose in this study, and it is a well studied linear algorithm, which is simple, straight forward and transparent. So it is selected for our further analysis.

The hypothesis of the logistic regression is

$$\mathbf{h} = g(\Lambda\theta) \tag{5}$$

where

$$g(\mathbf{z}) = \frac{1}{1+e^{-\mathbf{z}}} \tag{6}$$

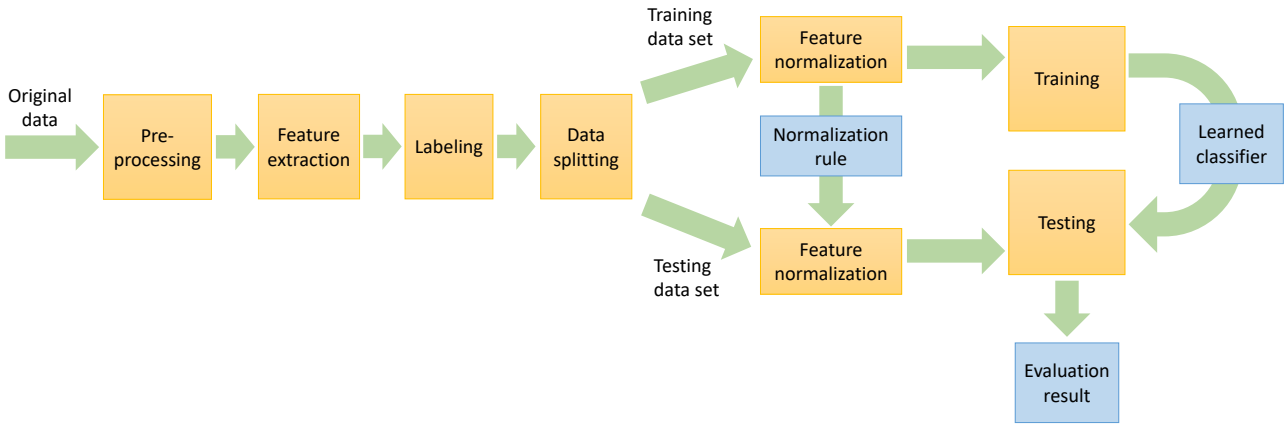

FIGURE 3. Work flow of detecting plunging breaking waves based on machine learning.

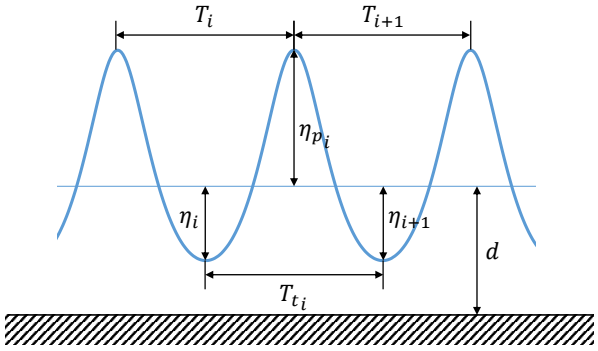

FIGURE 4. A representative time series of measured wave elevation.

is logistic function, in which

$$\mathbf{z} = \Lambda\theta \tag{7}$$

The matrix

$$\Lambda = \begin{bmatrix} 1 & \lambda_1^{(1)} & \lambda_2^{(1)} & \dots & \lambda_n^{(1)} \\ 1 & \lambda_1^{(2)} & \lambda_2^{(2)} & \dots & \lambda_n^{(2)} \\ \vdots & \vdots & \vdots & \ddots & \vdots \\ 1 & \lambda_1^{(m)} & \lambda_2^{(m)} & \dots & \lambda_n^{(m)} \end{bmatrix} \tag{8}$$

is composed of a column of ones and the normalized features $\lambda_j^{(i)}$, where $j = 1,2,...,n$ and $i = 1,2,...,m$.

$$\theta = \begin{bmatrix} \theta_0 & \theta_1 & \dots & \theta_n \end{bmatrix}^T \tag{9}$$

is the parameter vector of the hypothesis.

The cost function of logistic regression is

$$\mathbf{J}(\theta) = \frac{1}{m}\Big(-\mathbf{y}^T \log(\mathbf{h}) - (1-\mathbf{y})^T \log(1-\mathbf{h})\Big) \tag{10}$$

Since $m \gg n$ (The number of samples is much larger than the number of features), the trained model is not likely to be overfitted. Therefore, no regularization term is included in Eq. 10.

The parameter vector θ is estimated by minimizing the cost function. The Matlab function *fminunc* is used for the minimization.

Once the parameter vector is obtained, Eq. 5 can be used as the learned classifier to predict the results on new data sets. Given a threshold δ between 0 and 1, for $h \geq \delta$, the prediction p is 1, implying a plunging breaking wave; for $h < \delta$ the prediction p is 0, indicating a non-breaking wave. A typical value $\delta = 0.5$ is used in this study.

Testing

The learned classifier is applied to the feature normalized testing data set to make predictions. The predicted results are then compared to the actual labels for evaluation.

The first indicator of evaluation is accuracy, which is defined as the ratio of correct predictions to all predictions. The predicted results fall into four categories as shown in Fig. 5. Two more indicators of evaluation are defined based on the categories:

$$\text{Precision} = \frac{\text{True positives}}{\text{True positives} + \text{False positives}} \tag{11}$$

$$\text{Recall} = \frac{\text{True positives}}{\text{True positives} + \text{False negatives}} \tag{12}$$

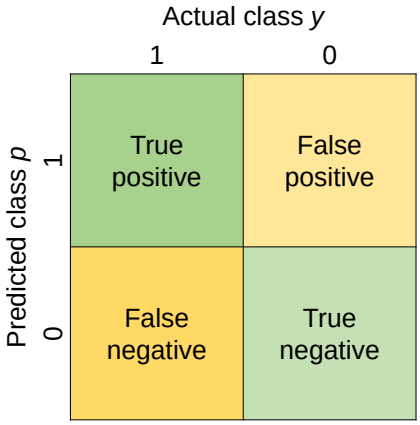

FIGURE 5. Four categories of the predicted results.

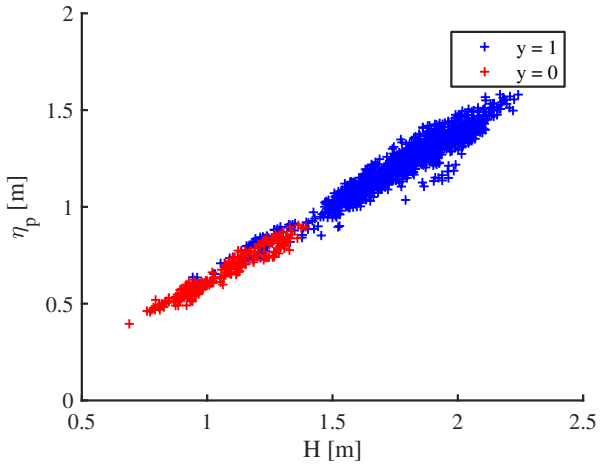

FIGURE 6. Measured wave height versus crest height for all samples. The blue and red color indicate breaking and non-breaking waves, respectively.

F_1 score is one way to combine precision and recall. It is defined as [14]

$$F_1 = 2\frac{\text{Precision} \times \text{Recall}}{\text{Precision} + \text{Recall}} \tag{13}$$

RESULTS AND DISCUSSIONS

Analysis of features

Scatter distributions of the extracted features are investigated in this section to identify representative features. Figs. 6 and 7 show the scatter plots of measured wave height versus crest height and trough height, respectively. Generally speaking, both the crest height and trough height vary linearly with the wave height for the considered regular waves. The linear behavior between the wave height and the crest height is better than that between the wave height and the trough height. The wave height H and crest height η_p are thus selected as representative features.

Figure 8 presents the scatter plot of estimated wave peak period and wave trough period for all samples. It can be found that the estimated wave peak periods usually deviate from the wave trough periods. Since the wave peaks are likely to be more accurately detected than the wave troughs from the measured time series, the wave peak period T_p is selected as another representative feature.

As a whole, four representative features, i.e. water depth d, wave height H, crest height η_p and wave peak period T_p, are used for further analysis. Three dimensionless features are derived from these four representative features, as follows:

$$x_1 = \frac{\eta_p}{H} \tag{14}$$

$$x_2 = \frac{H}{d} \tag{15}$$

$$x_3 = \sqrt{\frac{gT_p^2}{H}} \tag{16}$$

where g is the gravitational acceleration. These three dimensionless features (x_1, x_2, x_3) are then normalized to achieve three normalized dimensionless features, denoted by λ_1, λ_2 and λ_3, as described in the previous section. Hereinafter, the detection of plunging breaking waves are conducted with respect to λ_1, λ_2 and λ_3. From the training data set, the mean values and standard deviations of the three dimensionless features are estimated, as given in Table 3.

TABLE 3. The mean values μ and standard deviations σ of the three dimensionless features x_1, x_2 and x_3. They are calculated from the training data set and are used to calculate the corresponding normalized dimensionless features λ_1, λ_2 and λ_3 for both training set and testing set.

	μ	σ
x_1	0.675	0.036
x_2	0.846	0.168
x_3	11.567	1.639

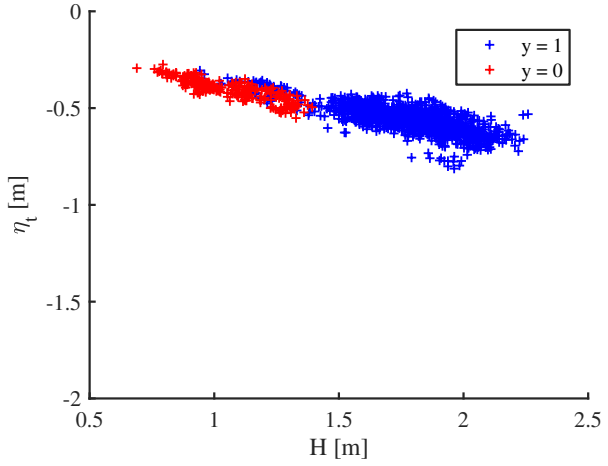

FIGURE 7. Measured wave height versus trough height for all samples. The blue and red color indicate breaking and non-breaking waves, respectively.

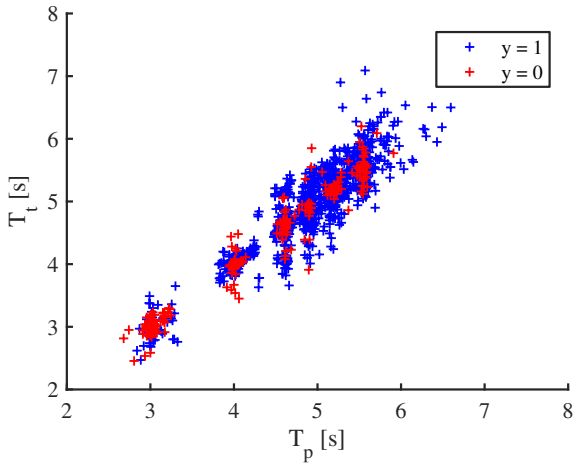

FIGURE 8. Measured wave peak period versus wave trough period for all samples. The blue and red color indicate breaking and non-breaking waves, respectively.

Parameter vector and decision boundary

The parameter vector θ is calculated by applying the training algorithm, and it is

$$\theta = \begin{bmatrix}\theta_0 & \theta_1 & \theta_2 & \theta_3\end{bmatrix}^T = \begin{bmatrix}8.591 & 1.819 & 6.330 & -1.571\end{bmatrix}^T \quad (17)$$

The parameter vector reveals the relative importance of λ_1, λ_2 and λ_3 on the hypothesis h, which indicates the probability of breaking. Among θ_1, θ_2 and θ_3, θ_2 has the highest absolute value, so λ_2 has the highest impact on h, which means that H/d is the most decisive factor for the breaking detection.

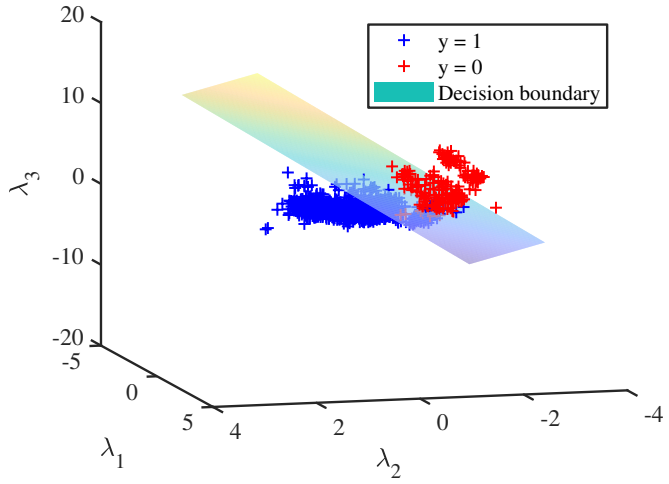

FIGURE 9. The decision boundary with training data set. The blue and red color indicate breaking and non-breaking waves, respectively.

The values θ_1 and θ_2 are both positive, so both λ_1 and λ_2 have a positive correlation with h. A larger value of λ_1 corresponds to a larger η_p/H, i.e. a more nonlinear wave, which is thus more likely to break. Breaking waves are more likely to occur in shallower water with a larger value of H/d. The value of θ_3 is negative, so λ_3 has a negative correlation with h. A larger value of λ_3 corresponds to a larger $\sqrt{\frac{gT_p^2}{H}}$, i.e. a more flat wave, which is less likely to break.

The parameter vector also gives the decision boundary of the classifier, as shown in Fig. 9. The decision boundary can be explicitly expressed as

$$z_\theta(\lambda) = 8.591 + 1.819\lambda_1 + 6.330\lambda_2 - 1.571\lambda_3 = 0 \quad (18)$$

When $z_\theta(\lambda) \geq 0$, prediction $p = 1$; when $z_\theta(\lambda) < 0$, prediction $p = 0$.

Inserting Eq. 3 to Eq. 18 with the values of μ and σ given in Table 3 and x_1, x_2, x_3 defined in Eqs. 14 to 16, we get

$$z_\theta(d,\eta_p,H,T_p) = 50.415\frac{\eta_p}{H} + 37.703\frac{H}{d} - 0.958\sqrt{\frac{gT_p^2}{H}} - 46.253 = 0 \quad (19)$$

The derived Eq. 19 can be directly applied to detect plunging breaking waves, once the four parameters (d,η_p,H,T_p) are known. According to Eq. 19, the (plunging) breaking criterion

can be written as

$$1.337\frac{\eta_p}{H}+\frac{H}{d}-0.025\sqrt{\frac{gT_p^2}{H}}-1.227\geq 0 \qquad (20)$$

Evaluation

For both training data set and testing data set, the labels are predicted by applying the learned classifier to the data. The predicted results p are evaluated against the given labels y. The evaluation results are summarized in Table 4 and visualized in Figs. 10 and 11. The evaluation results from the training set and the testing set are very similar, and the values of all the evaluation indicators are higher than 98%. So the learned classifier is neither overfitted nor underfitted. At least for the wave data with similar properties as the training data set, the classifier is reliable for the detection of plunging breaking waves.

The above results are obtained by using the threshold $\delta = 0.5$. The selection of the threshold can affect the predicted results. This effect can be illustrated by the receiver operating characteristic (ROC) curve [15], as shown in Fig. 12. The ROC curve shows the relationship between the true positive rate and the false positive rate that are calculated by using different thresholds. Ideally, a larger true positive rate and a smaller false positive rate are desired. However, they increase or decrease at the same time, when δ is changed. One needs to compromise between these two rates to get a reasonable classifier according to the application of the classifier. Since breaking waves are dangerous for offshore structures, a larger true positive rate is prioritized. Therefore, the classifier with the threshold $\delta = 0.5$ as marked in Fig. 12 seems reasonable for our purpose.

TABLE 4. Result evaluation. The results by the McCowan breaking criterion [16] are estimated for the testing data set.

	Training	Testing	McCowan criterion
True positive	1048	454	416
False positive	6	2	0
False negative	7	5	43
True negative	185	73	75
Accuracy	99.0%	98.7%	91.9%
Precision	99.4%	99.6%	100.0%
Recall	99.3%	98.9%	90.6%
F1 score	99.4%	99.2%	95.1%

The performance of the learned classifier is compared to that of the classical McCowan breaking criterion [16] (i.e. $H/d \geq$

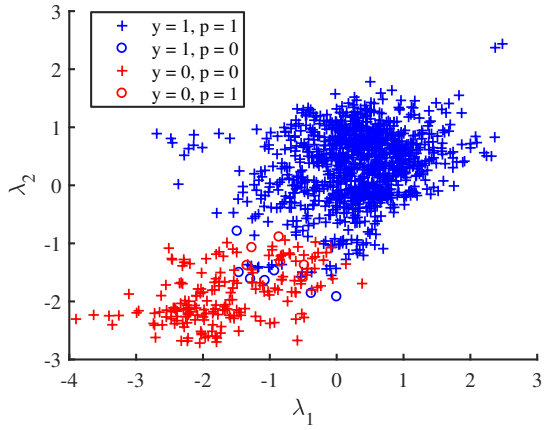

(a) λ_1 vs. λ_2

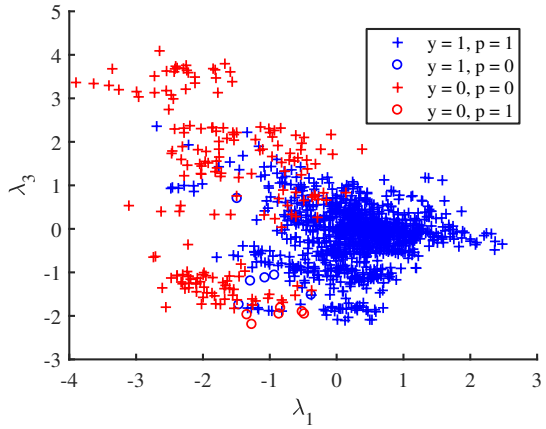

(b) λ_1 vs. λ_3

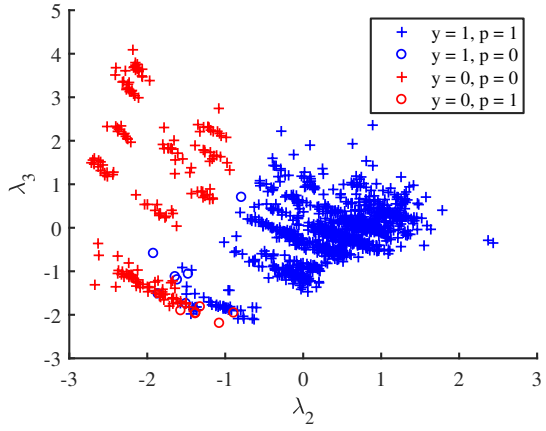

(c) λ_2 vs. λ_3

FIGURE 10. Evaluation result of the training data set shown in three directions. (a) λ_1 versus λ_2 (b) λ_1 versus λ_3 (c) λ_2 versus λ_3. The legend corresponds to four categories defined in Fig. 5.

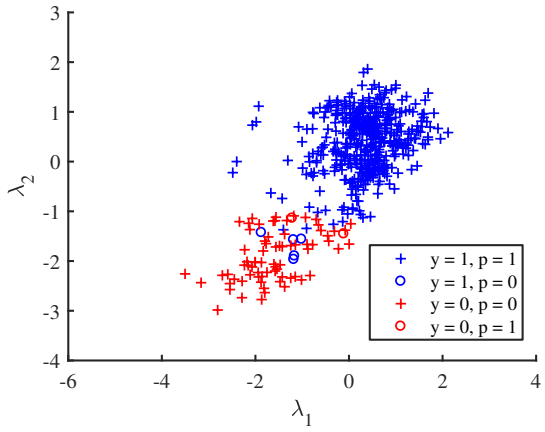

(a) λ_1 vs. λ_2

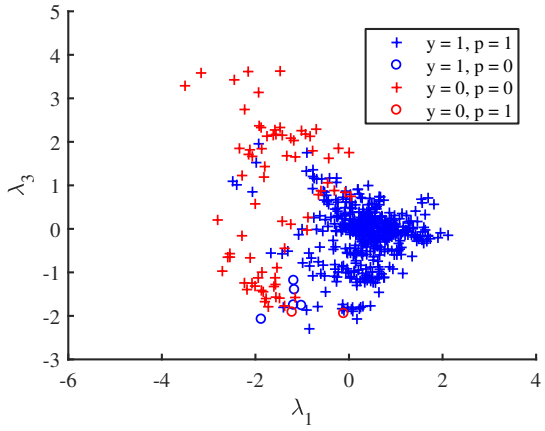

(b) λ_1 vs. λ_3

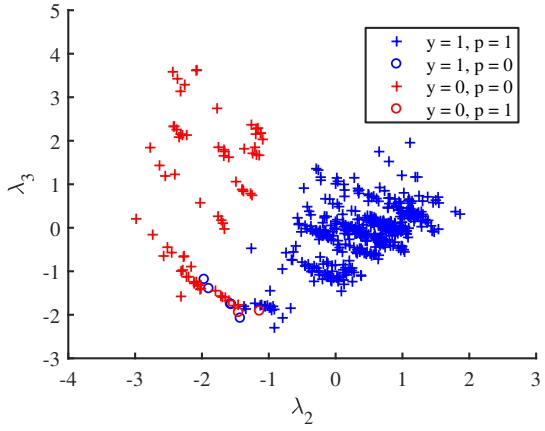

(c) λ_2 vs. λ_3

FIGURE 11. Evaluation result of the testing data set shown in three directions. (a) λ_1 versus λ_2 (b) λ_1 versus λ_3 (c) λ_2 versus λ_3. The legend corresponds to four categories defined in Fig. 5.

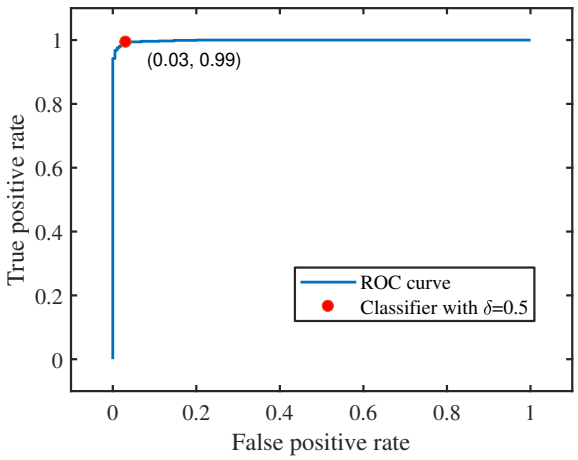

FIGURE 12. The receiver operating characteristic (ROC) curve (for training set only). The current classifier with the threshold $\delta = 0.5$ is marked on the curve.

0.78) with respect to the testing data set. The comparison is also given in Table 4. The precision of the breaking criterion is slightly higher than that of the learned classifier. However, the recall of the breaking criterion is lower by about 8%, which implies that a significant amount of breaking waves are not detected by the breaking criterion. The learned classifier has also a higher F_1 score, a higher accuracy and thus a better performance than the McCowan breaking criterion in general.

CONCLUSIONS

The detection of plunging breaking waves based on wave elevation data is investigated by using a supervised machine learning approach in this study.

The investigated problem is a typical binary classification problem. Based on a large amount of experimental data from the WaveSlam project, a classifier is trained by using logistic regression algorithm.

Three normalized dimensionless features are introduced based on the measured data for the training. A classifier with respect to four wave parameters (i.e. water depth, wave height, crest height and wave period) is then explicitly developed for detecting plunging breaking waves.

It is found that the learned classifier has an accuracy of 98.7% and F_1 score of 99.2% for the tested data. Among the three dimensionless parameters, the ratio of wave height to water depth, H/d, is the most decisive factor for the detection.

Compared to the classical McCowan breaking criterion, the learned classifier has a better performance that is indicated by a higher F_1 score, a higher accuracy and a higher recall.

More work should be done in the future to test the applica-

bility of the classifier under different wave conditions.

ACKNOWLEDGMENT

This work has been supported by the European Community's Seventh Framework Programme through the grant to the budget of the Integrating Activity HYDRALAB IV within the Transnational Access Activities, Contract no. 261520.

Financial support from NOWITECH FME (Research Council of Norway, contract no. 193823) is gratefully acknowledged.

REFERENCES

[1] Sarpkaya, T., and Isaacson, M., 1981. *Mechanics of wave forces on offshore structures*. New York: Van Nostrand Reinhold.

[2] Tu, Y., Cheng, Z., and Muskulus, M., 2017. "A review of slamming load application to offshore wind turbines from an integrated perspective". *Energy Procedia,* ***137***, pp. 346–357.

[3] Samuel, A. L., 1959. "Some studies in machine learning using the game of checkers". *IBM Journal of research and development,* ***3***(3), pp. 210–229.

[4] Witten, I. H., Frank, E., Hall, M. A., and Pal, C. J., 2016. *Data Mining: Practical machine learning tools and techniques*. Morgan Kaufmann.

[5] Kızılöz, B., Çevik, E., and Aydoğan, B., 2015. "Estimation of scour around submarine pipelines with artificial neural network". *Applied Ocean Research,* ***51***, pp. 241–251.

[6] Deo, M., and Naidu, C. S., 1998. "Real time wave forecasting using neural networks". *Ocean engineering,* ***26***(3), pp. 191–203.

[7] Zamani, A., Solomatine, D., Azimian, A., and Heemink, A., 2008. "Learning from data for wind–wave forecasting". *Ocean Engineering,* ***35***(10), pp. 953–962.

[8] Deo, M. C., Jha, A., Chaphekar, A., and Ravikant, K., 2001. "Neural networks for wave forecasting". *Ocean Engineering,* ***28***(7), pp. 889–898.

[9] Deo, M., and Jagdale, S., 2003. "Prediction of breaking waves with neural networks". *Ocean Engineering,* ***30***(9), pp. 1163–1178.

[10] Akoz, M. S., Cobaner, M., Kirkgoz, M. S., and Oner, A. A., 2011. "Prediction of geometrical properties of perfect breaking waves on composite breakwaters". *Applied Ocean Research,* ***33***(3), pp. 178–185.

[11] Kouvaras, N., and Dhanak, M. R., 2018. "Machine learning based prediction of wave breaking over a fringing reef". *Ocean Engineering,* ***147***, pp. 181–194.

[12] Arntsen, Ø., Obhrai, C., and Gudmestad, O., 2013. Data storage report: Wave slamming forces on truss structures in shallow water. WaveSlam (HylV-FZK-05), Technical Report, Norwegian University of Science and Technology.

[13] Ng, A., 2012. Machine learning: Logistic regression (week 3). Lecture notes from Coursera. Retrieved from: https://www.coursera.org/learn/machine-learning; March 2018.

[14] Powers, D. M., 2011. "Evaluation: from precision, recall and F-measure to ROC, informedness, markedness and correlation". *Journal of machine learning technologies,* ***2***(1), pp. 37–63.

[15] Fawcett, T., 2006. "An introduction to roc analysis". *Pattern recognition letters,* ***27***(8), pp. 861–874.

[16] McCowan, J., 1894. "On the highest wave of permanent type". *Philosophical Magazine Series 5,* ***38***(233), pp. 351–358.